


Continental tapering of South America caused asymmetric non-uniform opening of the South Atlantic Ocean

Dengliang Gao ¹ 

South Atlantic opening has been typically modelled as being related to symmetric and static thermal upwelling and seafloor spreading that drive divergent continental drift of South America and Africa. Comparative analyses, however, show that South Atlantic opening is asymmetric and non-uniform. For neither asymmetric nor non-uniform opening are the underlying mechanisms clear. Here I use geological and geophysical data to inform analytical modelling, revealing that westward drifting and southward tapering of the South American continent have controlled the asymmetry and the non-uniformity in South Atlantic opening. I interpret that the asymmetric non-uniform seafloor spreading caused the ridge and hotspots to migrate, leaving behind non-linear seamount trails that are indicative of the speed of hotspot migration rather than direction of plate movement. The findings point towards a chain reaction from continental drifting, through seafloor spreading to ridge-hotspot interaction, which is instrumental in understanding the geodynamics for global plate tectonics.

¹Department of Geology and Geography, West Virginia University, Morgantown, WV, USA. email: Dengliang.Gao@mail.wvu.edu

The South Atlantic Ocean has been a research hotspot for the geodynamics of continental drift and seafloor spreading^{1–8}. Since the Early Cretaceous^{3,4}, the South Atlantic has experienced the latest rift-drift cycle of the West Gondwana supercontinent without major tectonic overprinting. The young ocean basin is favorable for the preservation of geologic evidence for kinematic reconstruction. The young ocean basin is also favorable for making observations of footprints left by continental drift and seafloor spreading, making it possible to build and test models for South Atlantic opening. Thus, the South Atlantic serves as an ideal natural lab to conceive and test hypotheses for the geodynamics of global plate tectonics^{9–16}.

At the two conjugate margins of the South Atlantic, the pre-drift Lower Cretaceous section holds critical evidence left at the right time in the right place regarding how the South Atlantic opening kick-started. Unfortunately, reflection seismic data quality has been compromised underneath the Lower Cretaceous Aptian salt^{17–24}. The limitation of accessibility has left the Lower Cretaceous at the continental margins a blind spot where information on the origin of the South Atlantic Ocean remains covered. Many published seismic images only provide a vague picture of structural grains with questionable interpretations when it comes to the pre-drift Lower Cretaceous section. Eyeing on local variability with poor data quality without a big picture of the entire conjugate margins could lead to interpretational bias that deviates from the principle component of extensional tectonics.

Because the pre-drift deep section renders only a vague picture of rifts related to initial continental extension, interpretations of rift geometry are controversial and the origin of the rifted continental margins remains a topic of contentious debate. Basically, the previous art of interpretation for the pre-drift extension can be categorized into pure shear and simple shear models¹², with the former being accommodated by symmetric extension and the latter by asymmetric extension. Generally, many models depict the continental margin formation of the South Atlantic as being related to the South American and African Plates drifting away symmetrically from each other. Although previous studies have reported both the asymmetry and non-uniformity in the formation of South Atlantic conjugate margins^{6,7,15,25–31}, the underlying mechanism for neither asymmetric nor non-uniform continental rifting is well understood^{6,7}.

Beyond the continental margins, seafloor bathymetry, geomorphology and geochronology^{32–38} are typically interpreted as being related to a static spreading center and stationary hotspots. Among the most striking seafloor anomalies are the seamount chains that cross over seafloor flowlines (fracture zones). The trends of seamount chains have been used as a kinematic indicator for the South American and African Plates moving towards west and east, respectively^{33–38}. Although regional analyses of seafloor geology have shown both the asymmetry and non-uniformity in seafloor spreading^{10,29}, the underlying mechanism for neither asymmetric nor non-uniform seafloor spreading is clear.

The paucity of high-quality subsurface data and the deficiency in subsurface-surface data integration make it difficult to develop and test analytical models for the asymmetry and non-uniformity in South Atlantic opening. To address the problem, I have been updating the South Atlantic database (Fig. 1) by integrating seismic imagery, satellite free-air gravity, SeaBeam bathymetry and geochronology (see Methods). In particular, I have access to the latest pre-stack time- and depth-migrated seismic imagery of the deeply-buried, Lower Cretaceous section at both the Brazilian and Angolan margins. I reprocess the post-stack seismic signals to enhance the resolution of structural grains that have been previously difficult to image due to the frequency attenuation underneath the Lower Cretaceous Aptian salt. Informed by three-

dimensional comparative observations and interpretations, I perform analytical modeling to prove the concept in a quantitative manner. The observational and analytical results demonstrate that westward pull and southward tapering of the South American continent have been modulating early asymmetric rotational opening followed by late parallel opening of the South Atlantic Ocean. The findings suggest a chain reaction from continental drift, through seafloor spreading to ridge-hotspot interaction, which should have implications for the geodynamics of global plate tectonics.

Results

A geophysical jigsaw puzzle. The latest reflection seismic data offshore Brazil and Angola reveal contrasting rift structures between the two continental margins in the pre-drift Lower Cretaceous section (Fig. 2), which adds to previous seismic observations of rift geometry. The Brazilian margin¹⁸ is dominated by northeast-trending normal faults that dip to the east with large offset, whereas the Angolan margin²² is dominated by northwest-trending normal faults in association with westward-thickening depositional wedges atop westward-sloping basement ramps. The asymmetry is reflected by the depths of the basement, with the basement at the Brazilian margin being 1–5 km deeper than at the Angolan margin²⁴. The asymmetry is also reflected by the thicknesses of syn-rift clastics, carbonates and evaporites, with sediments at the Brazilian margin being 1–3 kilometers thicker than at the Angolan margin^{21,23}. The asymmetry is even reflected by the steepness of seaward-dipping reflectors (SDR's), with the SDR's at the Brazilian margin being 10°–20° steeper than at the Angolan margin³⁹. With the removal of the intervening ocean, the overall rift structures of the two continental margins could piece together into a large-scale asymmetric graben formed prior to the opening of the Ocean (Fig. 2).

In concert with seismic data, satellite free-air gravity^{25–27} also shows large-scale contrast in intensity and gradient between the Brazilian and the Angolan margins (Fig. 1; Supplementary Fig. 1), which is here interpreted as a gravity expression of a trans-Atlantic asymmetric graben. The Brazilian margin is dominated by high negative anomalies ranging from –30 to –65 mGal with a high gradient, whereas the Angolan margin is dominated by low negative or even positive anomalies ranging from –10 to +20 mGal with a low gradient. The gravity contrast extends consistently southwards to the Argentina and the Namibian margins. Isostatic anomalies indicate that the lithosphere is approximately 15 kilometers thinner and sediments approximately 3 kilometers thicker at the Argentina margin than at the Namibian margin²⁸.

Immediately above the contrasting basement structures are the contrasting detachment structures between the Brazilian and the Angolan margins (Fig. 2), suggesting a possible large-scale gravitational slide initiated during the rift-to-drift transition (Fig. 3). The Brazilian component¹⁸ is dominated by west-vergent folds and thrusts in association with a thick sequence of allochthonous salt, with salt bodies being stalled at east-dipping rift bumps. The Angolan component^{22,23} features west-dipping listric normal faults soling at a west-sloping detachment horizon of thin autochthonous salt, which transitions to west-vergent folds, thrusts and allochthonous salt towards west. The maximum fold curvature and the largest fault offset occur in the Lower Cretaceous below the break-up unconformity, suggesting that the gravitational sliding commenced as early as the Early Cretaceous prior to drift. Although the pre-drift west-bound gravitational slide was overprinted by passive-margin gravitational sliding in the drift phase, the initial gravitational slide of the Early Cretaceous can still be discernable and recoverable, with its toe

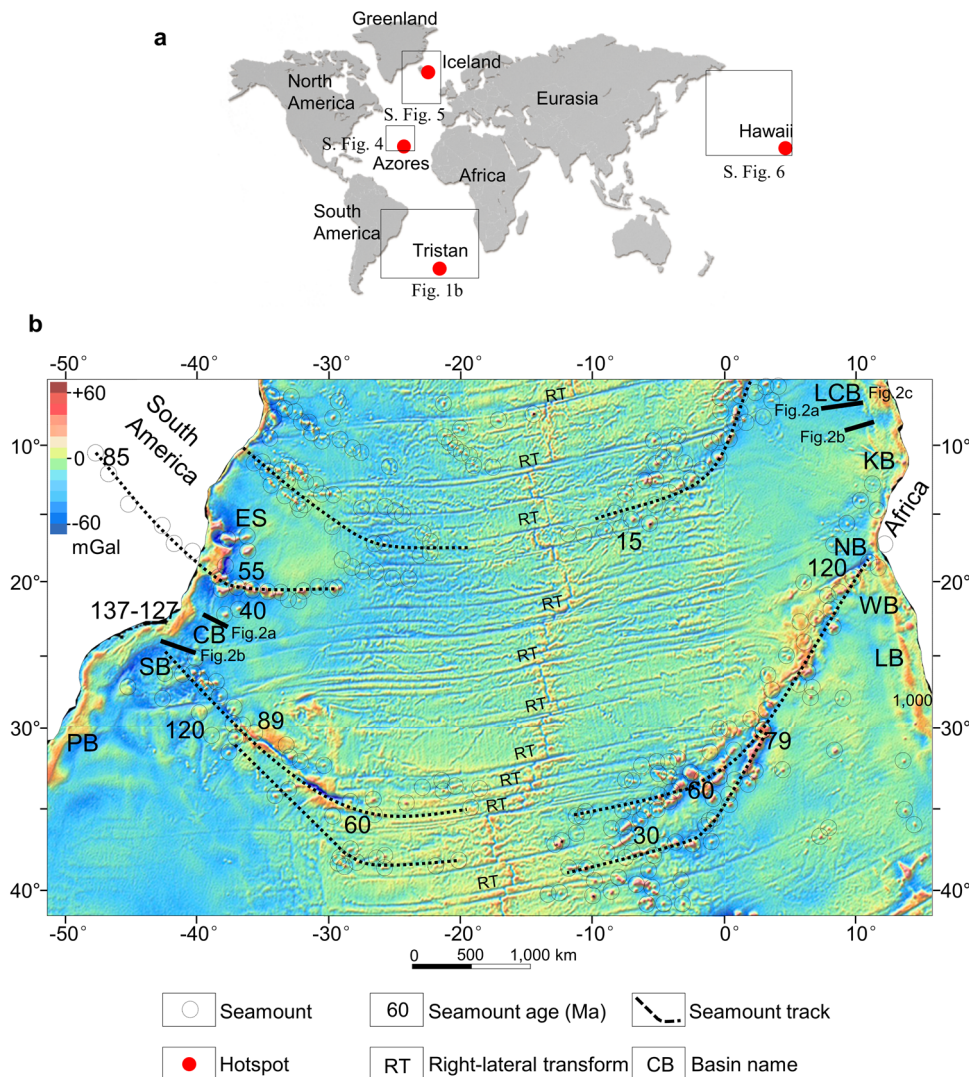


Fig. 1 An integrated data base of the South Atlantic Ocean. **a** Global location index map showing ocean basins and major hotspots discussed in this study. **b** South Atlantic Ocean base map. Color image shows satellite free-air gravity anomalies^{25,26}. Along the South American margin, large-scale negative anomalies widen from north to south. Along the Mid-Atlantic Ridge, positive anomalies show increases in width and amplitude from north to south, and are systematically segmented by right-lateral transform faults (RT). Bull's eye positive anomalies (circles) are seamounts²⁶ (Supplementary Fig. 1), and the numbers are seamount ages in m.y.^{26,32}. The seamounts are distributed along non-linear chains. The trends and ages of seamount chains change from north, where they cross over fracture zones when they are older, to south, where they bend towards fracture zones when they are younger. Seismic data used in this study cover the following basins at the conjugate margins: Pelotas Basin (PB), Santos Basin (SB), Campos Basin (CB), Espirito Santo Basin (ES), Lower Congo Basin (LCB), Kwanza Basin (KB), Namib Basin (NB), Walvis Basin (WB), and Luderitz Basin (LB).

(thrusts) in the Brazilian margin being split from its head (extensional faults) in the Angolan margin.

In association with the asymmetric graben and the gravitational slide are transfer faults at the Brazilian and the Angolan margins (Figs. 2 and 3), which have not been well documented previously because of the difficulty imaging vertical strike-slip faults. At both continental margins, transfer faults are vertically rooted in the basement^{21,23} and are laterally segmenting the rift system. Transfer faults at the Brazilian margin are dominantly trending northwest^{17,19–21}, whereas those at the Angolan margin are trending northeast²³. By rotating South America counterclockwise for approximately 50°, the Brazilian transfer faults and their Angolan counterparts are reunited into a northeast-trending, right-lateral transfer fault system. Following the initiation phase of South Atlantic opening, the two split sets of transfer faults drifted apart and were replaced by northeast-east-trending (80°) oceanic transform faults at approximately 120 Ma^{26,32}. An overwhelming majority (90%) of the transform faults show

right-lateral offset of the ridge, which is consistent with the offset of transfer faults at the continental margins.

Digital measurements of SeaBeam bathymetry^{29,30} of the South American and the African Atlantic uncover previously unknown geomorphologic patterns (Figs. 4–6; Supplementary Figs. 2, 3). The southward tapering of the South American continent correlates strongly to the width and depth of the South American Atlantic, whereas the correlation is weak in the African Atlantic (Figs. 5 and 6). Generally, the width of Mid-Atlantic Ridge is increasing toward the south (Fig. 5d). The cross-ridge depth profile shows that the western limb of the Mid-Atlantic Ridge is 1.5–2.0 times steeper than the eastern one (Fig. 7a), and the degree of the asymmetry increases towards south (Fig. 5d). The along-ridge depth profile³¹ sees asymmetric bulges, with their southern slopes being steeper than the northern one (Fig. 7b). Along the Mid-Atlantic Ridge, positive gravity ranges from +30 to +60 mGal and show along-ridge increases in both width and amplitude towards south. On both sides of the Ridge are

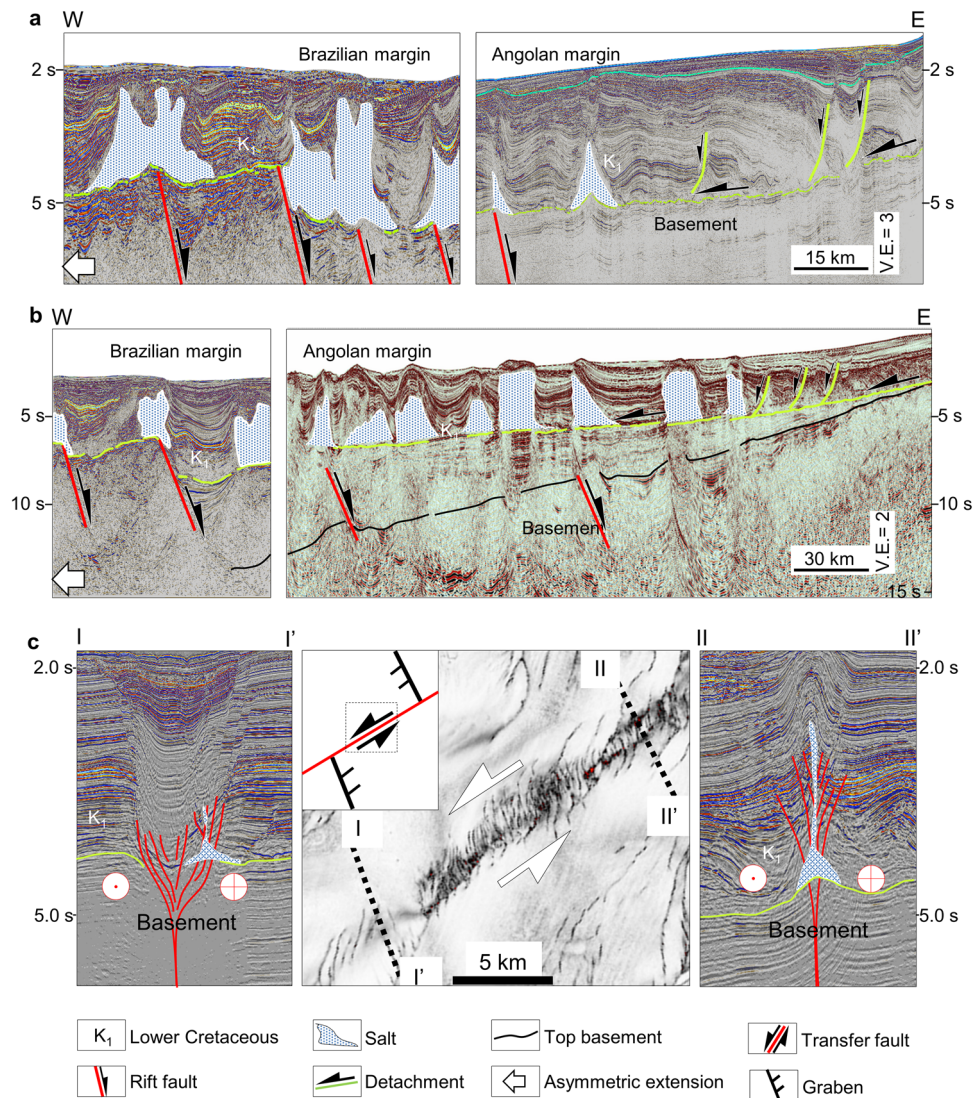


Fig. 2 Seismic image interpretations of a trans-Atlantic asymmetric graben, gravitational slide and transfer fault initially formed in the Early Cretaceous. The approximate locations of seismic lines are shown in Fig. 1b. **a** Type seismic sections focusing on detachment structures caused by gravitational sliding. **b** Type seismic sections focusing on asymmetric rift structures causing asymmetric subsidence and thickening of rift sediments. **c** A reactivated transfer fault at the Angolan continental margin, which is related to the northwest-trending rift faults. Seismic sections (I-I' and II-II') feature a negative flower structure (transtension) and a positive flower structure (transpression), respectively, both of which are kinematically consistent with the en-echelon pattern of fault traces.

asymmetrically distributed bird's eye gravity anomalies of seamounts (Fig. 1, Supplementary Fig. 1). Hundreds of seamounts are aligned along two sets of non-linear chains that converge towards south. The trends of seamount tracks are asymmetric about the spreading center, which is consistent with the excess accretion of oceanic crust on the South American Plate¹⁰. In the north, the seamounts do cross over but do not cross cut oceanic fracture zones (Fig. 4; Supplementary Fig. 1), indicating seamount chains are growing syn-tectonically from north to south across seafloor flowlines. As the seamounts become progressively younger towards south, they bend gradually towards the fracture zones (Figs. 1 and 4; Supplementary Fig. 1). Being consistent with the asymmetry of axial bulges related to live hotspots on the Mid-Atlantic Ridge, the southern slopes of seamounts off the Ridge are 3–4 times steeper than the northern ones (Figs. 4, 5e).

A hypothesis. Three-dimensional comparative observations of subsurface structural styles and surface morphological patterns do

not fit into previous models for continental drift, seafloor spreading and ridge-hotspot interaction in the South Atlantic. Instead, they hint at a genetic link between continental tapering of South America and asymmetric non-uniform opening of the South Atlantic Ocean (Figs. 8–10). In association with flood basalt eruption at pre-drift hotspots in the Early Cretaceous (137–120 Ma)^{1,3,26,32,40–42}, South Atlantic opening initiated with a large-scale asymmetric graben along with gravitational slides and transfer faults in West Gondwana. The splitting of the supercontinent to the tapering continent of South America set the initial boundary condition for South Atlantic opening.

Beginning with this initial boundary condition, analytical modeling offers a way to simulate how the South American continent has been manipulating the opening of the South Atlantic Ocean (see Methods). Analytical modeling results indicate that South Atlantic opening has actually experienced three distinct phases. The phased opening has been dynamically modulated by the southward tapering of the South American continent (Figs. 8–10).

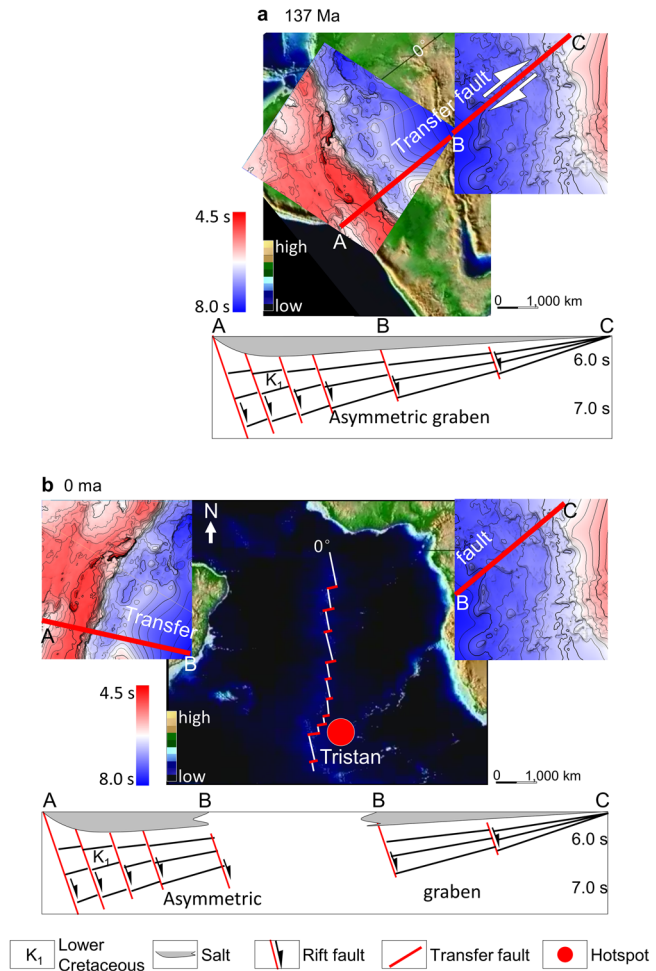


Fig. 3 An asymmetric graben and a transfer fault that split and drifted apart due to South Atlantic opening. The two contour maps are close-up views of the basement top derived from 3D seismic surveys at the Brazilian and the Angolan margins, respectively. **a** Pre-drift configuration of an asymmetric graben and a transfer fault. **b** Present-day configuration of the graben and the transfer fault.

In phase one (t_1), with no accretion of oceanic crust, asymmetric non-uniform continental rifting and intra-continental shearing are expressed by Eqs. (1) and (2), respectively (see Methods):

$$D(y, t) = \frac{(f - r)t^2}{2\rho_c k_c w_c(y)} \quad (1)$$

$$\lambda(y, t) = -\frac{(f - r)t^2}{2\rho_c k_c w_c(y)^2} \frac{dw_c(y)}{dy} \quad (2)$$

where $D(y, t)$ and $\lambda(y, t)$ are drift and shear strain, respectively; y is longitudinal location, and t is time; f and r are driving and resistance force, respectively; ρ_c and k_c are continental density and thickness, respectively; $w_c(y)$ is continental width. The equations state that the change in continental width is controlling continental rotation and shearing. Numerical simulation (see Methods) shows that southward decrease in width of the South American continent causes southward increase in continental extension, leading to right-lateral shearing and clockwise rotation of continent (Fig. 9). In the south where continental width is small, drift is swift, whereas in the north where continental width

is large, drift is sluggish. The magnitude and sense of shear are both dictated by the continental width gradient. The difference between southern swift and northern sluggish rifting is provable with reported extensional velocities¹⁵.

In phase two (t_2), with accretion of oceanic crust, the width of plate increases with time, and the asymmetric non-uniform continental drifting and shearing are expressed by the Eqs. (3) and (4), respectively (see Methods):

$$D(y, t) = \int_0^t \left[\int_0^t \frac{f - r}{\rho_c k_c w_c(y) + \rho_o k_o w_o(y, t)} dt \right] dt \quad (3)$$

$$\lambda(y, t) = \frac{\partial}{\partial y} \left[\int_0^t \left[\int_0^t \frac{f - r}{\rho_c k_c w_c(y) + \rho_o k_o w_o(y, t)} dt \right] dt \right] \quad (4)$$

where ρ_o and k_o are oceanic density and thickness, respectively; $w_o(y, t_2)$ is oceanic width. The equations state that the width of both continental and oceanic crust jointly control the continental drift, seafloor spreading and intra-plate shearing. Since the tapering continent is incrementally accreted by the oceanic crust, the incremental drift $D_i(y, t_2)$ and incremental shear $\lambda_i(y, t_2)$ are derived as numerical solutions to Eqs. (3) and (4) by using Eqs. (5) and (6), respectively (see Method):

$$D_i(y, t) = \frac{(f - r)t^2}{2[\rho_c k_c w_c(y) + \rho_o k_o w_o(y, t_2)]} \quad (5)$$

$$\lambda_i(y, t) = -\frac{(f - r)t^2}{2[\rho_c k_c w_c(y) + \rho_o k_o w_o(y, t_2)]^2} \left[\rho_c k_c \frac{dw_c(y)}{dy} + \rho_o k_o \frac{\partial w_o(y, t_2)}{\partial y} \right] \quad (6)$$

which show that as the width of plate increases and the width gradient of plate decreases, the rates for plate rotation and intra-plate shearing decrease with time (Figs. 8 and 10).

In phase three (t_3), with the tapering continent being fully compensated by proportional accretion of oceanic crust, Eqs. (5) and (6) become Eqs. (7) and (8), respectively (see Methods):

$$D_i(y, t) = \frac{(f - r)t^2}{2m(t)} \quad (7)$$

$$\lambda_i(y, t) = 0 \quad (8)$$

where $m(t)$ is a composite function of width and density of both continental and oceanic crust, the equations state that the incremental drift becomes uniform and incremental shear is zero, in which case oceanic opening becomes non-rotational and no intra-plate shearing occurs as typically observed along oceanic fracture zones (Figs. 8 and 10).

Test of hypothesis. Seafloor bathymetry, geomorphology and geochronology in the South Atlantic offer blind tests and cross validations for the proposed model. In response to the asymmetric continental drift, the South Atlantic seafloor has been spreading more aggressively towards west than towards east¹⁰, as indicated by the asymmetry of the continental margins, the ocean basins and the Mid-Atlantic Ridge. In association with asymmetric seafloor spreading, the Mid-Atlantic Ridge has been drifting westwards¹⁰, which explains its western limb being steeper than the eastern one. In response to clockwise rotation and right-lateral shearing of South America, the continental margin, the ocean basins and the Mid-Atlantic Ridge all widen southwards. The scissor opening would induce southward propagation of decompression plume, driving hotspots to migrate from north to south. As the hotspots migrate along the spreading center, the pre-existing hotspots split and drift sideways along seafloor flowlines, leaving behind two sets of fossil

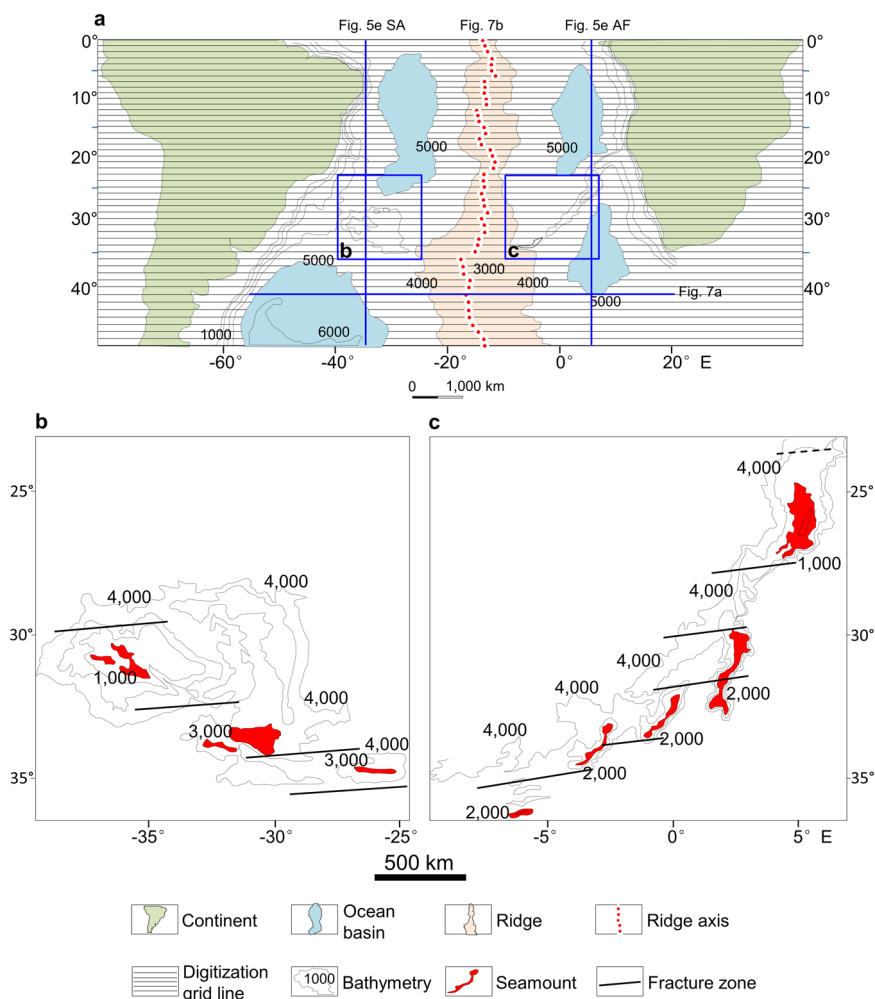


Fig. 4 Gridded contour maps for digitization of bathymetric elements in the South Atlantic³⁵. **a** Up-scaled contour map (contour interval = 1000 m) overlaid with east-west grid lines at an interval = 1° latitude along which width and depth of bathymetric elements are digitized and plotted. Width measured along east-west gridlines carry a systematic error of -3% to +3% compared to the width measured along the oceanic transform faults and continental transfer faults. The digitized results are shown in Figs. 5–7. **b** Down-scaled contours of the Rio Grande Rise. **c** Down-scaled contours of the Walvis Ridge.

hotspot tracks as coupled seamount chains that converge towards south, or as singled seamount chains if the migrating hotspot is off the ridge. The southward migrating hotspots explain the asymmetric axial bulges (live hotspots) and off-axis seamounts (fossil hotspots) that have steeper southern slopes than the northern ones. The southward migrating hotspots also explain the cross-over but not cross-cutting relation of seamount chains to fracture zones. The apparent (pseudo) offset of the seamounts across fracture zones is indicative of the along-ridge migration of existing (live) hotspots and cross-ridge drift of pre-existing (fossil) hotspots along seafloor flowlines. So, hotspot tracks are not indicative of movement direction of plates, neither are they indicative of movement direction of hotspots. Instead, they are indicative of migration speed of hotspots along the Mid-Atlantic Ridge. The cross-over angle of hotspot tracks with fracture zones is a measure of hotspot migration velocity, and the bend of hotspot tracks is indicative of slow-down in hotspot migration. The change is expected because, as demonstrated in analytical modeling (see Method), the continental tapering effect on rotational opening waned over time with non-uniform accretion of oceanic crust, which steer scissor opening to parallel opening, causing migrating hotspots to stall and seamount chains to bend.

Discussion

The South Atlantic model can be extended to the North Atlantic to offer insights into the underlying mechanism for the asymmetric non-uniform opening of the North Atlantic Ocean^{33,34,43–50} (Supplementary Fig. 4). Likewise, the North American continent and the Mid-Atlantic Ridge have both been proactively drifting away from the African and Eurasian continent^{43–46}. In association with the southward tapering of the North American continent, the Ocean widens southwards and the Ridge con-occurs with right-lateral transform faults. Located approximately 100 miles east of the Mid-Atlantic Ridge, the Azores hotspot is associated with seamounts that are distributed asymmetrically about the Mid-Atlantic Ridge^{47,48}. The seamount chains converge toward south and cross over fracture zones. The hotspot was reported to have been migrating along the Mid-Atlantic Ridge^{33,34,49,50}, but the migration direction has been controversial^{34,49} and the underlying mechanism has been puzzling. All these can be well explained by the South Atlantic model. The model predicts that continental tapering of North America controlled asymmetric non-uniform opening of the North Atlantic Ocean and along-ridge migration of the Azores hotspot.

The South Atlantic model can also be extended to the northernmost North Atlantic to offer insights into the mechanism for

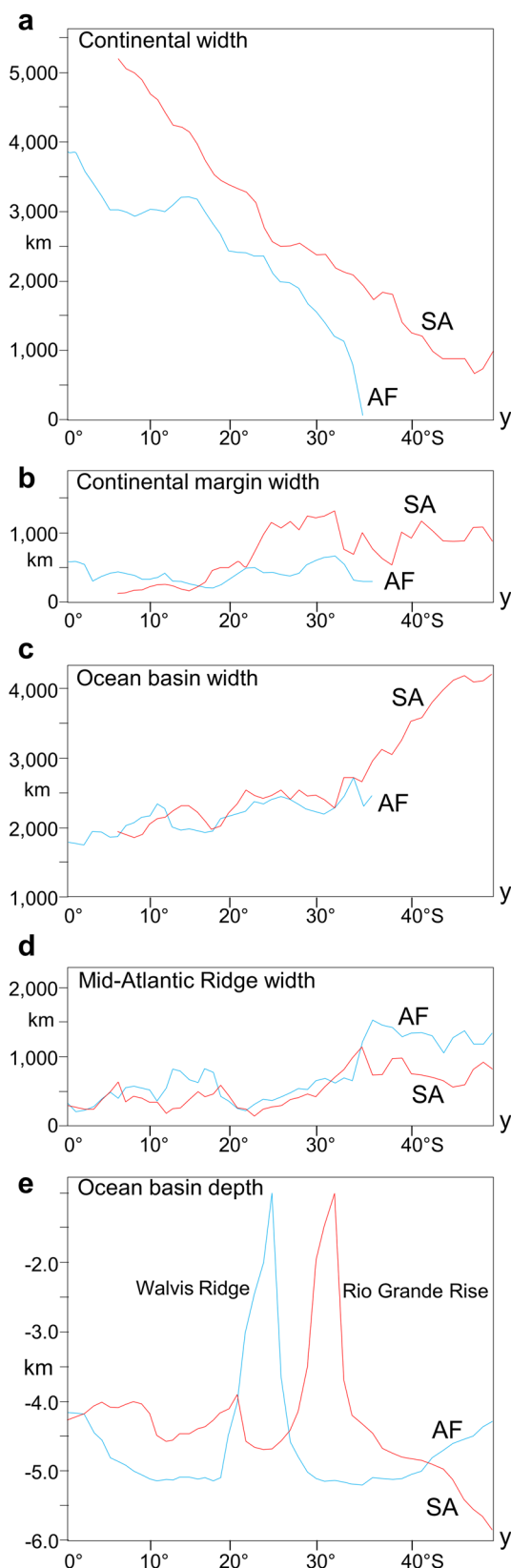


Fig. 5 Longitudinal variations and latitudinal contrasts in width and depth of bathymetric elements of the South American (SA) and the African (AF) Plates. Data are derived from the gridded contour maps (Fig. 4) and are plotted against latitude. The original base map and data samples are shown in Supplementary Figs. 2, 3, respectively. **a** Width of the South American continent in red and the African continent in blue (bathymetry = 0 m). **b** Width of the South American continental margin in red and the African continental margin in blue (bathymetry 0–4000 m). **c** Width of the South American Atlantic Ocean basin in red and the African Atlantic Ocean basin in blue (bathymetry > 4000 m). **d** Width of the South American Mid-Atlantic Ridge in red and the African Mid-Atlantic Ridge in blue (bathymetry < 4000 m). **e** Depth of the South American Atlantic (longitude = 34°30'W) in red and the African Atlantic (longitude = 5°50'E) in blue.

Ridge is flanked by southward convergent seamounts and troughs that cross over fracture zones. All these characteristics can be explained by extrapolating the South Atlantic model to the northernmost Atlantic Ocean. The South Atlantic model predicts that the northernmost Atlantic Ocean has been opening slowly and the Iceland hotspot migrating sluggishly with reduced degree of asymmetry because the northernmost Atlantic Ocean is associated with the widest continents at the northernmost end of the tapering continent of North America.

The South Atlantic model can be further extended to the Pacific Ocean and offers a different perspective for the origin of the Hawaiian-Emperor seamount chain than previous models^{57–62} (Supplementary Fig. 6). The famous bend of the seamount chain (Supplementary Fig. 6a) has been widely used as a classical example of change in movement direction of the Pacific Plate^{59,60} or the Hawaiian hotspot^{61,62}; however, three kinematic and dynamic issues remain unresolved for the 60° change in direction of the Pacific Plate motion or mantle flow. First, the seamount chain is crossing over seafloor flowlines, which requires simultaneous seafloor spreading and displacement of the Pacific Plate in different directions. Second, the Musicians seamount chain in the same north-central portion of the Pacific Plate shows a different orientation along with a different bending angle of 80° than the Hawaiian-Emperor chain, which requires the same portion of a plate to move in kinematically conflict directions at the same time. Third, although many geologic models attempt to prove the concept of change in movement direction of the Pacific Plate or mantle flow, the lack of an analytical model makes it hard to explain why and how the Pacific Plate or the mantle flow suddenly changed the course. Yet, the South Atlantic model provides a simple mechanism to resolve the dilemmas. According to the South Atlantic model, the 60° bend of the seamount chain is not necessarily indicative of a 60° change in movement direction of neither the Pacific Plate nor the Hawaiian hotspot. Rather, the bend is indicative of slow-down of the Hawaiian hotspot migration, or speed-up of the Pacific seafloor spreading. The slow-down of the Hawaiian hotspot can be attributable to the non-uniformity in seafloor spreading that is typical of oceanic opening, whereas the speed-up of seafloor spreading can be attributable to the subduction initiation of the Pacific Plate at its western margin at 50 Ma⁵⁸.

The findings in this study provide a long-sought-after analytical solution to the underlying mechanism for asymmetric diachronous continental margin formation, asymmetric non-uniform seafloor spreading and non-static thermal upwelling in the South Atlantic and other ocean basins. The mechanism hints at a chain reaction from continental drift, through seafloor spreading to ridge-hotspot interaction. The chain reaction undermines the classical theory of thermal convection and upwelling as active drivers for global plate tectonics.

along-axis variations in asymmetry and non-uniformity in Atlantic opening that have been contentious^{51–56} (Supplementary Fig. 5). Located near the southward tapering continent of Greenland where the Atlantic Ocean is the narrowest, the Iceland hotspot sits only 5 miles east of the Mid-Atlantic Ridge. The Ridge is consistently segmented by right-lateral transform faults with small offset. The

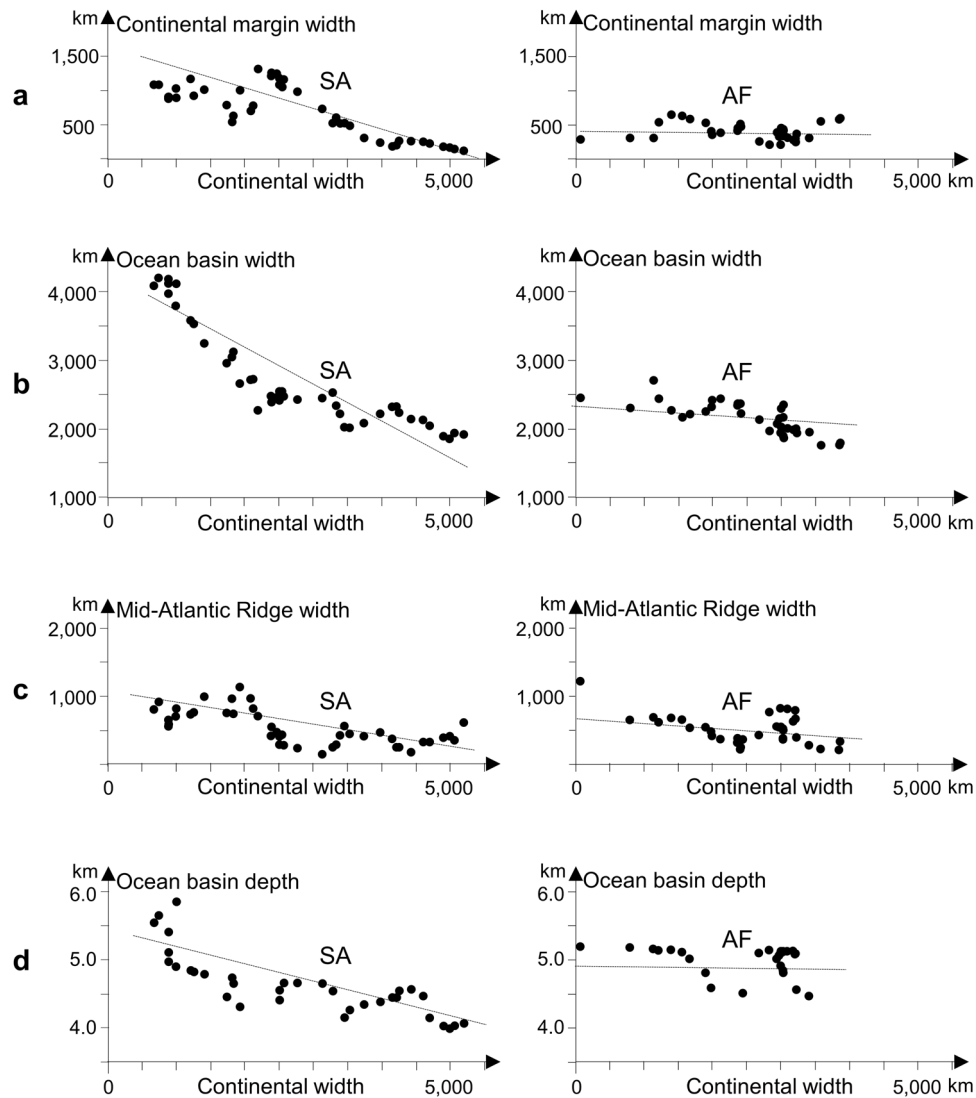


Fig. 6 Cross-correlations of continental width to bathymetry in the South American (SA) and the African (AF) Atlantic. The original base map and data samples are shown in Supplementary Figs. 2, 3, respectively. Note the South American continent (left) has a much higher correlation to bathymetry than the African continent (right). **a** Continental margin width cross plotting with continental width of South America (left) and Africa (right). **b** Ocean basin width cross plotting with continental width of South America (left) and Africa (right). **c** Mid-Atlantic Ridge width cross plotting with continental width of South America (left) and Africa (right). **d** Ocean basin depth cross plotting with continental width of South America (left) and Africa (right). Anomalous depth samples at the Rio Grande Rise and the Walvis Ridge are removed to better represent the regional depth trend.

Methods

Data integration. Tens of thousands of square kilometers of three-dimensional surveys and thousands of kilometers of two-dimensional seismic lines are accessed for this study in the Brazilian Campos and Santos Basins and in the Angolan Kwanza and Lower Congo Basins. The seismic source wave reaches kilometers below the sea floor to the Lower Cretaceous basement, uncovering evidence formed immediately before the drift and in the vicinity of the piercing line at the continent-ocean boundary. The amplitude signals are digitized with 4-miliseconds sampling rate in vertical dimension and in 100 by 100 feet grids of inlines and crosslines. The signals are processed by seismic service contractors using pre-stack time migration algorithms. Following the pre-stack time migration, I apply a post-stack seismic amplitude waveform analysis algorithm coded in C++ to visualize subsurface structures⁶³. The pre-stack and post-stack processing add to the quality of subsurface data sets in the South Atlantic database^{21,23}. In particular, the processed seismic images help reveal basement structural details underneath the Lower Cretaceous Aptian salt which have been poorly imaged in previous seismic surveys.

After seismic data processing, I begin with seismic image analysis in the Brazilian Santos and Campos Basins and in the Angolan Kwanza and Lower Congo Basins. I target pre-drift structures below the Lower Cretaceous Aptian salt, searching for geologically unique geometric and kinematic indicators of continental rift and drift. I am particularly interested in pre-salt rift and transfer faults and post-salt but pre-drift gravitational slides below the break-up unconformity. Using

computer-aided interactive volume visualization and digital mapping software Petrel© developed by Schlumberger, I take a three-dimensional comparative approach to recover pre-salt rift geometry and post-salt detachment structural style between the two conjugate margins. I extend the comparative investigation along both margins from north to south to evaluate the consistency and variability in rifts, gravitational slides, and transfer faults.

Next, I incorporate high-resolution free-air gravity data from RADAR ALTIMETRY²⁵ at http://topex.ucsd.edu/marine_grav/mar_grav.html to complement seismic data analysis. A continuous coverage of gravity data provides geophysical basis for objective extrapolation of structural grains in areas with either poor seismic image quality or scarce seismic coverage. The gravity data also serve to filter out small-scale variabilities shown in high-frequency seismic imagery. In addition, free-air gravity anomalies help highlight seafloor morphologic features such as seamounts and seamount chains. To paint a regional picture of structural, geomorphological and thermal anomalies, I systematically compare satellite free-air gravity anomalies between the South American and African Atlantic margins in order to explore their correlation to subsurface seismic imagery. I translate gravity intensity map into a series of gravity intensity profiles perpendicular to the rifted margins and integrate them with seismic data to define rift structures in the pre-salt Lower Cretaceous section. I choose type seismic lines and gravity profiles at the corresponding locations in order to tie seismic time structures with gravity anomalies. Using the focus areas with high-density, high-quality seismic data as the

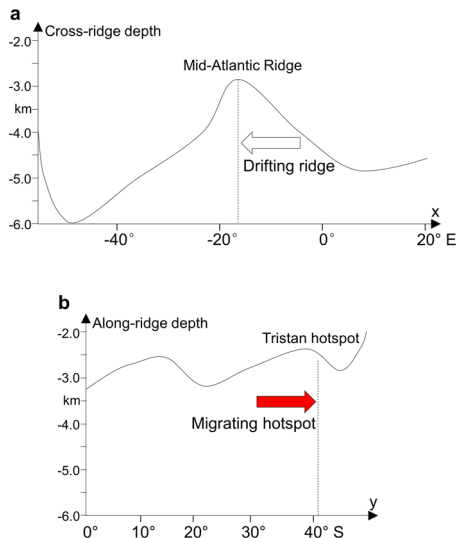


Fig. 7 Depth profiles across and along the axis of the Mid-Atlantic Ridge. See Fig. 4 for locations. **a** Depth profile across the axis of the Mid-Atlantic Ridge showing asymmetric Atlantic Ocean and Mid-Atlantic Ridge. **b** Depth profile³¹ along the axis of the Mid-Atlantic Ridge showing asymmetric axial bulges.

training grounds, I extrapolate the gravity-seismic joint interpretations along the two continental margins in order to define the rift geometry of the Lower Cretaceous section in the subsurface.

Then, using data analysis software, I digitize SeaBeam bathymetric data from GLOBAL TOPOGRAPHY³⁰ at http://topex.ucsd.edu/marine_grav/mar_grav.html in the greater South Atlantic region. I quality check bathymetric maps for digitization by using latitude-longitude grid lines. I partition the South Atlantic into the South American Atlantic and African Atlantic for comparative analysis. To characterize continental tapering, I measure the width between the eastern and western coastlines along east-west grid lines at an interval of 1° of latitude. I take the coastlines (bathymetry = 0 meter) instead of the continent-ocean boundary because of the ambiguity and uncertainty in delineating the boundary. Below the sea level, I digitize the widths and depths of the two conjugate continental margins, ocean basins, and the Mid-Atlantic Ridge. I then run cross plots between continental width and bathymetry for both South American and African Atlantic. Using bathymetry and free-air gravity anomalies, I mark hundreds of seamounts and define their trends. I am particularly interested in the cross-over relations of seamounts to fracture zones and the change in cross-over angle (obliquity) of seamount chains relative to fracture zones.

I collect geochronological data^{26,32} to constrain the ages of volcanics and seafloor. After quality-checking the geochronologic data obtained using different methods, I note error and uncertainty and even inconsistency in absolute geologic time from different sources. So I use the chronologic data as a reference rough time frame only for the growth history of seamounts and seamount chains.

Finally, I conceive a hypothetical model and develop analytical modeling based on geophysical rules without major speculations of driving parameters. Based on analytical models, I perform numerical experimentation and simulation. I test the hypothesis using independent observational data that are not directly involved in analytical modeling and numerical simulation. I extend and test the model developed in the South Atlantic to the North Atlantic and Pacific Ocean.

Analytical modeling. The analytical models are here presented with reduced variability and dimensionality for the demonstration of the concept that the tapering continent of South America modulates the asymmetry and the non-uniformity in South Atlantic opening. The modeling is extendable to three dimensions with additional variables, but the reduced-order modeling results do not compromise the quality of the conclusions.

To begin with analytical modeling, I set up a Cartesian coordinate system with x and y axes pointing to east and south, respectively. I put into the system the South American continent and measure continental width in x direction as a function of y . I create a dynamic model with time t as a variable to characterize the phased opening of the South Atlantic Ocean.

First, in phase one (t_1) when no oceanic crust has accreted to the continent, I derive Eqs. (9) through (11) to model continental extension based on Newton’s law of motion:

$$a(y, t) = \frac{f - r}{\rho_c k_c w_c(y)} \tag{9}$$

$$v(y, t) = 0 \int_0^t \frac{f - r}{\rho_c k_c w_c(y)} dt = \frac{(f - r)t}{\rho_c k_c w_c(y)} \tag{10}$$

$$D(y, t) = \int_0^t \left[\int_0^t \frac{f - r}{\rho_c k_c w_c(y)} dt \right] dt = \int_0^t \frac{(f - r)t}{2\rho_c k_c w_c(y)} dt = \frac{(f - r)t^2}{2\rho_c k_c w_c(y)} \tag{11}$$

where $a(y, t)$, $v(y, t)$ and $D(y, t)$ are acceleration, velocity, and finite drift distance, respectively; f and r are driving and resistance force, respectively, and net force ($f-r$) is set to be a constant for focused demonstration of concepts and analytical solutions to the equations; ρ_c and k_c are continental density and thickness, respectively; $w_c(y)$ is continental width.

By taking the partial derivative of $D(y, t)$, I derive Eq. (12) to model intra-continental shearing of potential transfer faults:

$$\lambda(y, t) = \frac{\partial}{\partial y} \left[\frac{(f - r)t^2}{2\rho_c k_c w_c(y)} \right] = - \frac{(f - r)t^2}{2\rho_c k_c w_c(y)^2} \frac{dw_c(y)}{dy} \tag{12}$$

where $\lambda(y, t)$ is finite shear strain that is controlled by the along-strike variation in continental width $w_c(y)$.

Using Eqs. (11) and (12), I conduct numerical simulation for continental rifting and shearing, respectively (Supplementary Data 1). I take digital measurements of South America width along latitude grids at a 1° interval from north to south. The inputs for the simulation are continental density ρ_c , continental thickness k_c and digitized continental width $w_c(y)$ (Supplementary Table 1).

Second, in phase two (t_2) when continental crust is incrementally accreted by newly generated oceanic crust, the analytical modeling becomes a dynamic one because continental width is incrementally accreted by oceanic width. Again based on Newton’s law of motion, I derive Eqs. (13) through (15) to model continental drift and seafloor spreading:

$$a(y, t) = \frac{f - r}{\rho_c k_c w_c(y) + \rho_o k_o w_o(y, t)} \tag{13}$$

$$v(y, t) = \int_0^t \frac{f - r}{\rho_c k_c w_c(y) + \rho_o k_o w_o(y, t)} dt \tag{14}$$

$$D(y, t) = 0 \int_0^t \left[\int_0^t \frac{f - r}{\rho_c k_c w_c(y) + \rho_o k_o w_o(y, t)} dt \right] dt \tag{15}$$

where ρ_o and k_o are oceanic density and thickness, respectively; $w_o(y, t)$ is oceanic width.

By taking the partial derivative of $D(y, t)$, I derive Eq. (16) to model shearing of potential oceanic transform faults:

$$\lambda(y, t) = \frac{\partial}{\partial y} \left[\int_0^t \left[\int_0^t \frac{f - r}{\rho_c k_c w_c(y) + \rho_o k_o w_o(y, t)} dt \right] dt \right] \tag{16}$$

where $\lambda(y, t)$ is shear strain that is controlled by the along-strike variation in combined width of both continental and oceanic crust.

In the case of phase two, when the width is not constant but is variable with time t , I seek numerical solution instead of analytical one to the Eqs. (15) and (16) in order to estimate incremental drift $D_i(y, t)$ and incremental shear $\lambda_i(y, t)$ by using Eqs. (17) and (18), respectively:

$$D_i(y, t) = \frac{(f - r)t^2}{2[\rho_c k_c w_c(y) + \rho_o k_o w_o(y, t_2)]} \tag{17}$$

$$\lambda_i(y, t) = \frac{\partial}{\partial y} \left[\frac{(f - r)t^2}{2[\rho_c k_c w_c(y) + \rho_o k_o w_o(y, t_2)]} \right] = - \frac{(f - r)t^2}{2[\rho_c k_c w_c(y) + \rho_o k_o w_o(y, t_2)]^2} \left[\rho_c k_c \frac{dw_c(y)}{dy} + \rho_o k_o \frac{\partial w_o(y, t_2)}{\partial y} \right] \tag{18}$$

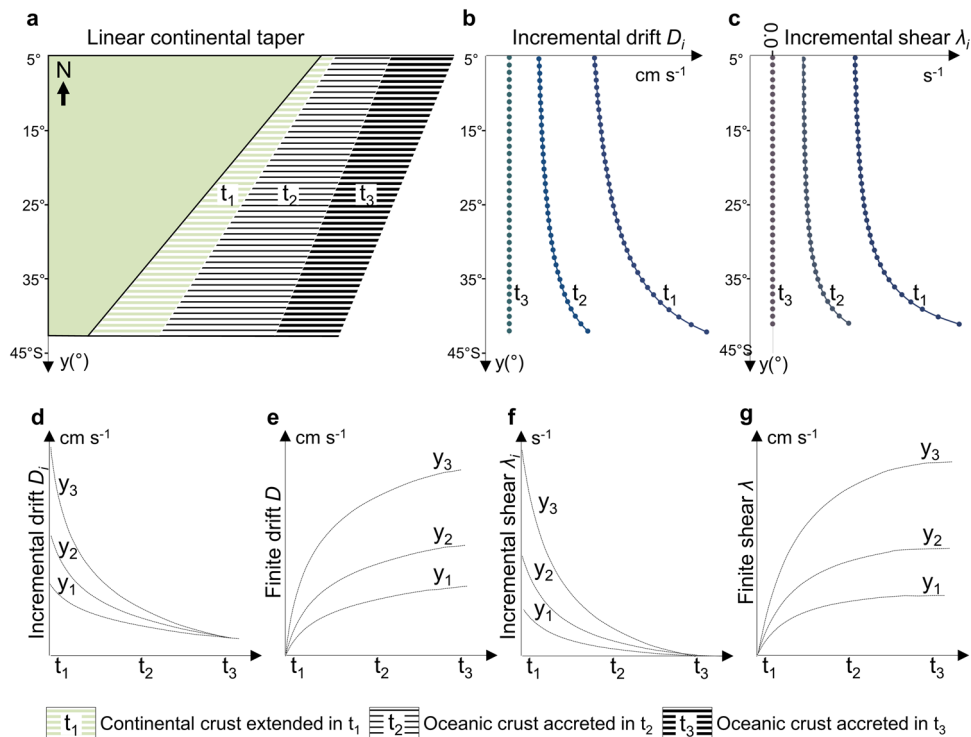
Using Eqs. (17) and (18), I conduct numerical simulation for seafloor spreading and shearing, respectively (Supplementary Data 2). The inputs are digitized continental width $w_c(y)$, continental density ρ_c and continental thickness k_c , oceanic density ρ_o and oceanic thickness k_o (Supplementary Table 2). The oceanic width $w_o(y, t)$ is dynamically updated with each time increment.

Finally, when the tapering continent is fully compensated by proportionally accreted oceanic crust, the simulation transits to phase three (t_3), and Eqs. (17) and (18) become Eqs. (19) and (20), respectively:

$$D_i(y, t) = \frac{(f - r)t^2}{2m(t)} \tag{19}$$

$$\lambda_i(y, t) = \frac{\partial}{\partial y} \left[\frac{(f - r)t^2}{2m(t)} \right] = 0 \tag{20}$$

where $m(t)$ is a function of t but not y . The equations explicitly state that continental drift eventually becomes uniform with no intra-plate shearing and oceanic opening becomes non-rotational.



Not to scale

Fig. 8 Schematic diagram demonstrating a linear continental taper modulating phased oceanic opening. See Methods and Supplementary Tables 1, 2 and Supplementary Data 1, 2 for reference. **a** A linear continental taper, with width decreasing linearly from north to south, is extended in phase one (t_1) and then accreted by oceanic crust in phase two (t_2) and phase three (t_3). **b** Incremental drift $D_i(y, t)$ as a function of y . In phase one (t_1) and phase two (t_2), drift increases from north to south, whereas in phase three (t_3) drift becomes uniform. **c** Incremental shear $\lambda_i(y, t)$ as a function of y . In phase one (t_1) and phase two (t_2), shear increases from north to south, whereas in phase three (t_3) shear becomes zero. **d** Incremental drift $D_i(y, t)$ as a function of t at three latitudes y_1, y_2 and y_3 . **e** Finite (accumulative) drift $D(y, t)$ as a function of t at three latitudes y_1, y_2 and y_3 . **f** Incremental shear $\lambda_i(y, t)$ as a function of t at three latitudes y_1, y_2 and y_3 . **g** Finite (accumulative) shear $\lambda(y, t)$ as a function of t at three latitudes y_1, y_2 and y_3 .

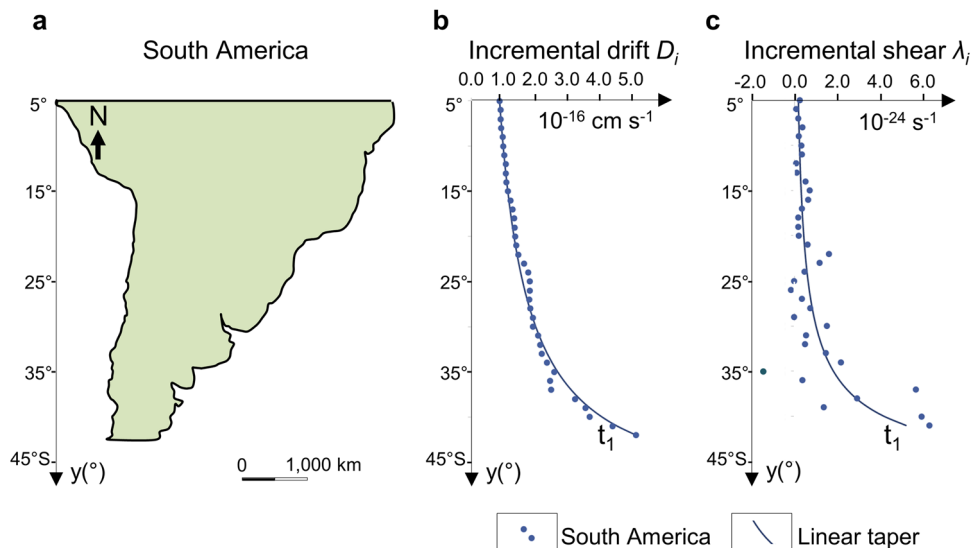


Fig. 9 Analytical modeling and numerical simulation results showing southward increasing drift and right-lateral shear of the tapering continent of South America during the initial phase (t_1). See Methods and Supplementary Table 1 for inputs and outputs, and Supplementary Data 1 to replicate the simulation. Incremental drift and shear are both plotted against latitude along the y -axis. The dots are calculated results from the non-linear taper of the South American continent. The curves are calculated results from a linear taper with the average tapering angle of the South American continent. As the South American continental width decreases from north to south, drift and shear increase, causing clockwise rigid rotation and intraplate right-lateral shear deformation. **a** Tapering continent of South America with its width decreasing non-linearly from north to south. **b** Incremental drift $D_i(y, t)$ in the initial phase (t_1). **c** Incremental shear $\lambda_i(y, t)$ in the initial phase (t_1). Note an overwhelming majority of shear strain is positive (right-lateral) because overall continental width decreases from north to south.

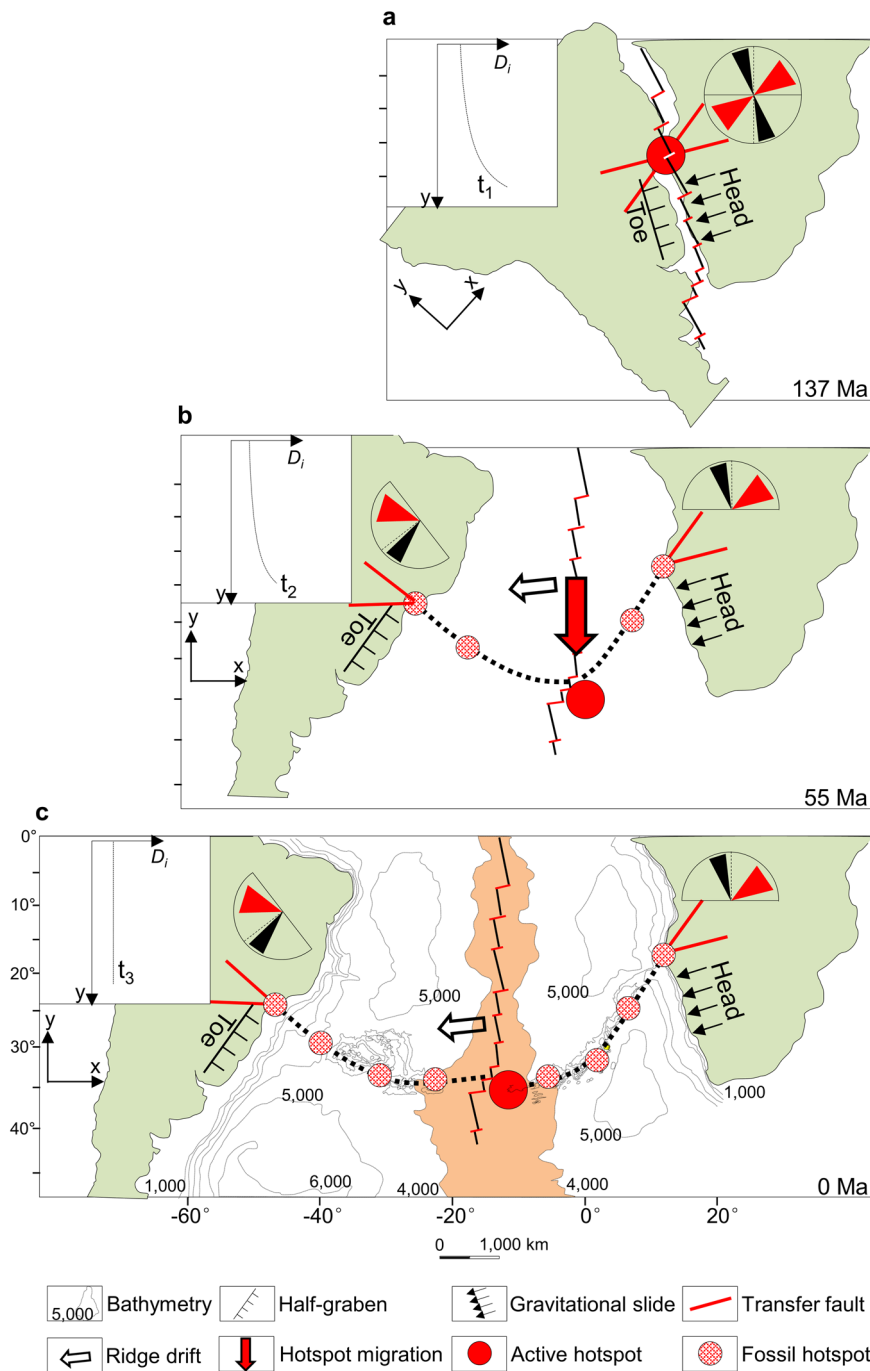


Fig. 10 Dynamic phased opening of the South Atlantic Ocean modulated by continental tapering of South America. The present-day outlines of the South American continent, South Atlantic Ridge and transforms are used to schematically demonstrate the concept because they have actually experienced intra-continental shear deformation along with rotation. **a** At approximately 137 Ma, South Atlantic opening began with an asymmetric graben, a gravitational slide and transfer faults. The rose diagram denotes the original orientations of rift faults (black) and transfer faults (red). **b** From approximately 137 Ma to 55 Ma, southward tapering of the South American continent caused right-lateral shear along with clockwise rotation of the continent, leading to southward scissor opening of the Ocean. The southward increase in spreading rate induced southward propagation of decompression plume, driving live hotspots to migrate from north to south and leaving behind two split chains of fossil hotspots that cross over seafloor flowlines. The rose diagrams denote the split and rotated rift faults (black) and transfer faults (red). **c** Since approximately 55 Ma, as the effect of continental tapering has waned due to proportional accretion of the oceanic crust, continental drift and seafloor spreading have become non-rotational, causing migrating hotspots to stall and seamount chains to bend.

Data availability

Free-air gravity and SeaBeam bathymetric data are obtained from RADAR ALTIMETRY and GLOBAL TOPOGRAPHY, respectively at http://topex.ucsd.edu/marine_grav/mar_grav.html. The input and output data for analytical modeling and numerical experimentation are available in Supplementary Data 1, 2 embedded with coded

analytical equations. Industry-owned raw seismic data used in this study are available in the Figshare open access repository at <https://doi.org/10.6084/m9.figshare.c.6244950.v3>.

Code availability

The C++ codes used in this study are freely available from the corresponding author upon request.

Received: 21 September 2021; Accepted: 14 October 2022;

Published online: 11 November 2022

References

- Wegener, A. *Die Entstehung der Kontinente und Ozeane* 23, 94, (Friedrich Vieweg & Sohn, Braunschweig, 1915).
- Bullard, E., Everett, J. E. & Smith, A. G. The fit of the continents around the Atlantic. *Philos. Trans. R. Soc. London A Math. Phys. Eng. Sci.* **258**, 41–51 (1965).
- Larson, R. L. & Ladd, J. W. Evidence for the opening of the South Atlantic in the Early Cretaceous. *Nature* **246**, 209–212 (1973).
- Nürnberg, D. & Müller, R. D. The tectonics of the South Atlantic from late Jurassic to present. *Tectonophysics* **191**, 27–53 (1991).
- Torsvik, T. H., Rouse, S., Labails, C. & Smethurst, M. A. A new scheme for the opening of the South Atlantic Ocean and the dissection of an Aptian salt basin. *Geophys. J. Int.* **177**, 1315–1333 (2009).
- Blaich, O. A., Faleide, J. I. & Tsikalas, F. Crustal breakup and continent-ocean transition at South Atlantic conjugate margins. *J. Geophys. Res. Solid Earth* **116**, B01402 (2011).
- Beniast, A., Willingshofer, E., Sokoutis, D. & Sassi, W. Extending continental lithosphere with lateral strength variations: effects on deformation localization and margin geometries. *Front. Earth Sci.* **6**, 148 (2018).
- Granot, R. & Dymant, J. The Cretaceous opening of the South Atlantic Ocean. *Earth Planet. Sci. Lett.* **414**, 156–163 (2015).
- Lister, G. S., Etheridge, M. A. & Symonds, P. A. Detachment models for the formation of passive continental margins. *Tectonics* **10**, 1038–1064 (1991).
- Muller, R. D., Roest, W. R. & Royer, J.-Y. Asymmetric sea-floor spreading caused by ridge-plume interactions. *Nature* **396**, 455–459 (1998).
- Ranero, C. R. & Perez-Gussinye, M. Sequential faulting explains the asymmetry and extension discrepancy of conjugate margins. *Nature* **468**, 294–299 (2010).
- Untermeier, P., Peron-Pinvidic, G., Manatschal, G. & Sutra, E. Hyper-extended crust in the South Atlantic: in search of a model. *Pet. Geosci.* **16**, 207–215 (2010).
- Heine, C., Zoethout, J. & Muller, R. D. Kinematics of the South Atlantic rift. *Solid Earth* **4**, 215–253 (2013).
- Pérez-Díaz, L. & Eagles, G. Constraining South Atlantic growth with seafloor spreading data. *Tectonics* **33**, 1848–1873 (2014).
- Brune, S., Heine, C., Pérez-Gussinye, M. & Sobolev, S. V. Rift migration explains continental margin asymmetry and crustal hyper-extension. *Nat. Commun.* **5**, 4014 (2014).
- Brune, S., Williams, S. E., Butterworth, N. P. & Müller, R. D. Abrupt plate accelerations shape rifted continental margins. *Nature* **536**, 201–204 (2016).
- Untermeier, P., Curie, D., Olivet, J. L., Goslin, J. & Beuzart, P. South Atlantic fits and intraplate boundaries in Africa and South America. *Tectonophysics* **155**, 169–179 (1988).
- Chang, H. K., Kowmann, R. O., Figueiredo, A. M. F. & Bender, A. Tectonics and stratigraphy of the east Brazil rift system: an overview. *Tectonophysics* **213**, 97–138 (1992).
- Jacques, J. M. A tectonostratigraphic synthesis of the sub-Andean basins: Inferences on the position of South American intraplate accommodation zones and their control on South Atlantic opening. *J. Geol. Soc. London* **160**, 703–717 (2003).
- Oreiro, S. G., Cupertino, J. A., Szatmari, P. & Thomaz Filho, A. Influence of pre-salt alignments in post-Aptian magmatism in the Cabo Frio High and its surroundings, Santos and Campos Basins, SE Brazil: An example of non-plume-related magmatism. *J. South Am. Earth Sci.* **25**, 116–131 (2008).
- Gao, D. et al. Intra-slope northwest-trending lineaments and geologic implications in the central Campos basin, offshore Brazil. In: *AAPG International Conference and Exhibition, Rio de Janeiro, Brazil* (American Association of Petroleum Geologists, 2009).
- Hudec, M. R. & Jackson, M. P. A. Regional restoration across the Kwanza basin, Angola: Salt tectonics triggered by repeated uplift of a metastable passive margin. *AAPG Bull.* **88**, 971–990 (2004).
- Gao, D., & Milliken, J. Cross-regional intraslope lineaments on the Lower Congo Basin Slope, offshore Angola (west Africa): Implications for tectonics and petroleum systems at passive continental margins. In: *Tectonics and sedimentation: Implications for petroleum systems: AAPG Memoir* **100**, (ed. Gao, D.) 229–248 (American Association of Petroleum Geologists, 2012).
- Koopmann, H., Schreckenberger, B., Franke, D., Becker, K. & Schnabel, M. The late rifting phase and continental break-up of the southern South Atlantic: the mode and timing of volcanic rifting and formation of earliest oceanic crust. *Geological Society, London, Special Publications* **420**, 315–340 (2014).
- Sandwell, D. T. & Smith, W. H. F. Geosat Altimetry gravity and topography/bathymetry: 1 min, Scripps Institution of Oceanography, UC SAN DIEGO, http://topex.ucsd.edu/marine_grav/mar_grav.html (2008).
- Meisling, K. E., Cobbold, P. R. & Mount, V. S. Segmentation of an obliquely rifted margin, Campos and Santos basins, south-eastern Brazil. *AAPG Bull.* **85**, 1903–1924 (2001).
- Dragoi-Stavar, D. & Hall, S. Gravity modeling of the ocean-continent transition along the South Atlantic margins. *J. Geophys. Res.* **114**, B09401 (2009).
- Shahraki, M., Schmeling, H. & Haas, P. Lithospheric thickness jumps at the S-Atlantic continental margins from satellite gravity data and modelled isostatic anomalies. *Tectonophysics* **722**, 106–117 (2018).
- Flament, N. et al. Topographic asymmetry of the South Atlantic from global models of mantle flow and lithospheric stretching. *Earth Planet. Sci. Lett.* **387**, 107–119 (2014).
- Pérez-Díaz, L. & Eagles, G. South Atlantic paleobathymetry since early Cretaceous. *Sci. Rep.* **7**, 11819 (2017).
- Stanton, N. S. G., Mello, S. L. M., Maia, M., Sichel, S. E., & de Souza, L. E. M. South Atlantic Ridge segmentation. In: *The 8th International Congress of The Brazilian Geophysical Society held in Rio de Janeiro, Brazil* (The Brazilian Geological Society, 2003).
- Turner, S., Regelous, M., Kelley, S., Hawkesworth, C. & Mantovani, M. Magmatism and continental break-up in the South Atlantic: high precision ⁴⁰Ar-³⁹Ar geochronology. *Earth Planet. Sci. Lett.* **121**, 333–348 (1994).
- Vogt, P. R. Global magmatic episodes: new evidence and implications for the steady-state mid-oceanic ridge. *Geology* **7**, 93–98 (1979).
- Arnould, M., Ganne, J., Coltice, N. & Feng, X. Northward drift of the Azores plume in the Earth's mantle. *Nat. Commun.* **10**, 3235 (2019).
- O'Connor, J. M. & Duncan, R. A. Evolution of the Walvis Ridge–Rio Grande Rise hotspot system: Implication for African and South American plate motions over plumes. *J. Geophys. Res.* **95**, 17475–17502 (1990).
- Schilling, J. G., Thompson, G., Kingsley, R. & Humphris, S. Hotspot-migrating ridge interaction in the South Atlantic. *Nature* **313**, 187–191 (1985).
- Brozena, J. & White, R. Ridge jumps and propagations in the South Atlantic Ocean. *Nature* **348**, 149–152 (1990).
- O'Connor, J. M. et al. Hotspot trails in the South Atlantic controlled by plume and plate tectonic processes. *Nat. Geosci.* **5**, 735–738 (2012).
- Reuber, K., Mann, P. & Pindell, J. Hotspot origin for asymmetrical conjugate volcanic margins of the austral South Atlantic Ocean as imaged on deeply penetrating seismic reflection lines. *Interpretation* **7**, SH71–SH97 (2019).
- VanDecar, J., James, D. & Assumpção, M. Seismic evidence for a fossil mantle plume beneath South America and implications for plate driving forces. *Nature* **378**, 25–31 (1995).
- Fromm, T. et al. South Atlantic opening: a plume-induced breakup? *Geology* **43**, 931–934 (2015).
- Morgana, J. P., Taramón, J. M., Araujo, M., Hasenclever, J. & Perez-Gussinye, M. Causes and consequences of asymmetric lateral plume flow during South Atlantic rifting. *PNAS* **117**, 27877–27883 (2020).
- Steinberger, B., Sutherland, R. & Connell, R. J. O. Prediction of Emperor-Hawaii seamount locations from a revised model of global plate motion and mantle flow. *Nature* **430**, 167–173 (2004).
- Torsvik, T. H., Müller, R. D., Van Der Voo, R., Steinberger, B. & Gaina, C. Global plate motion frames: toward a unified model. *Rev. Geophys.* **46**, RG3004 (2008).
- Dobrovine, P. V., Steinberger, B. & Torsvik, T. H. Absolute plate motions in a reference frame defined by moving hot spots in the Pacific, Atlantic, and Indian oceans. *J. Geophys. Res.* **117**, 9101 (2012).
- Schilling, J.-G. Fluxes and excess temperatures of mantle plumes inferred from their interaction with migrating mid-oceanic ridges. *Nature* **352**, 397–403 (1991).
- Gente, P., Dymant, J., Maia, M. & Goslin, J. Interaction between the Mid-Atlantic Ridge and the Azores hot spot during the last 85Myr: Emplacement and rifting of the hot spot-derived plateaus. *Geochem. Geophys. Geosyst.* **4**, 1–23 (2003).
- Lourenco, N. et al. Morpho-tectonic analysis of the Azores Volcanic Plateau from a new bathymetric compilation of the area. *Marine Geophys. Res.* **20**, 141–156 (1998).
- Cannat, M. et al. Mid-Atlantic Ridge–Azores hotspot interactions: along-axis migration of a hotspot-derived event of enhanced magmatism 10 to 4 Ma ago. *Earth Planet. Sci. Lett.* **173**, 257–269 (1999).
- Steinberger, B. Plumes in a convecting mantle: models and observations for individual hotspots. *J. Geophys. Res.* **105**, 11127–11152 (2000).
- Vogt, P. R. Asthenosphere motion recorded by the ocean floor south of Iceland. *Earth Planet. Sci. Lett.* **13**, 153–160 (1971).
- Sandwell, D. & Smith, W. H. F. Marine gravity from Geosat and ERS-1 altimetry. *J. Geophys. Res.* **102**, 10039–10054 (1997).
- Ito, G. Reykjanes ‘V’-shaped ridges originating from a pulsing and dehydrating mantle plume. *Nature* **411**, 681–684 (2001).

54. Hey, R., Martinez, F., Höskuldsson, Á. & Benediktsdóttir, Á. Propagating rift model for the V-shaped ridges south of Iceland. *Geochem. Geophys. Geosyst.* **11**, Q03011 (2010).
55. Martinez, F. & Hey, R. Propagating buoyant mantle upwelling on the Reykjanes Ridge. *Earth Planet. Sci. Lett.* **457**, 10–22 (2017).
56. Howell, S. M. et al. The origin of the asymmetry in the Iceland hotspot along the Mid-Atlantic Ridge from continental breakup to present-day. *Earth Planet. Sci. Lett.* **392**, 143–153 (2014).
57. Sandwell, D. T. & Smith, W. H. F. Global marine gravity from retracked Geosat and ERS-1 altimetry: Ridge segmentation versus spreading rate. *J. Geophys. Res.* **114**, B01411 (2009).
58. O'Connor, J. M. et al. Deformation-related volcanism in the Pacific Ocean linked to the Hawaiian–Emperor bend. *Nat. Geosci.* **8**, 393–397 (2015).
59. Sharp, W. D. & Clague, D. A. 50-Ma Initiation of Hawaiian–Emperor bend records major change in Pacific Plate motion. *Science* **313**, 1281–1284 (2006).
60. Domeier, M. et al. Intraoceanic subduction spanned the Pacific in the Late Cretaceous–Paleocene. *Sci. Adv.* **3**, eao2303 (2017).
61. Tarduno, J. A. et al. The Emperor Seamounts: Southward motion of the Hawaiian hotspot plume in Earth's mantle. *Science* **301**, 1064–1069 (2003).
62. Horner-Johnson, B. C. & Gordon, R. G. True polar wander since 32 Ma B. P.: a paleomagnetic investigation of the skewness of magnetic anomaly 12r on the Pacific Plate. *J. Geophys. Res.* **115**, B09101 (2010).
63. Gao, D. Latest developments in seismic texture analysis for subsurface structure, facies, and reservoir characterization: a review. *Geophysics* **76**, W1–W13 (2011).

Acknowledgements

SINOPEC, Marathon Oil, Maersk Oil, Andes Petroleum Ecuador, WesternGeco, Occidental Petroleum, Schlumberger and other institutions granted permission to use their proprietary and public seismic, satellite free-air gravity, digital elevation and SeaBeam bathymetric data, making it possible to build and update an integrated database for this study. Thanks to T. Duan, Z. Feng, W. Zhang, Z. Liu, M. Li, J. Milliken, L. Seidler, D. Quirk, D. Hsu, R. Holt, F. Yang, Q. Hu, D. Good, A. Taday, X. Zhang and many others for their logistical help in accessing data. Schlumberger offered Petrel® and Ocean® software license for seismic data analysis. This study is a contribution to the West Virginia University Geophysics Consortium.

Author contributions

D.G. conceived the scientific concept, performed data collection, processing and interpretation, developed and implemented analytical modeling and numerical simulation, and wrote the paper.

Competing interests

The authors declare no competing interests.

Additional information

Supplementary information The online version contains supplementary material available at <https://doi.org/10.1038/s43247-022-00587-3>.

Correspondence and requests for materials should be addressed to Dengliang Gao.

Peer review information *Communications Earth & Environment* thanks Anouk Beniest and the other, anonymous, reviewer(s) for their contribution to the peer review of this work. Primary Handling Editors: Derya Gürer, Joe Aslin.

Reprints and permission information is available at <http://www.nature.com/reprints>

Publisher's note Springer Nature remains neutral with regard to jurisdictional claims in published maps and institutional affiliations.



Open Access This article is licensed under a Creative Commons Attribution 4.0 International License, which permits use, sharing, adaptation, distribution and reproduction in any medium or format, as long as you give appropriate credit to the original author(s) and the source, provide a link to the Creative Commons license, and indicate if changes were made. The images or other third party material in this article are included in the article's Creative Commons license, unless indicated otherwise in a credit line to the material. If material is not included in the article's Creative Commons license and your intended use is not permitted by statutory regulation or exceeds the permitted use, you will need to obtain permission directly from the copyright holder. To view a copy of this license, visit <http://creativecommons.org/licenses/by/4.0/>.

© The Author(s) 2022